Postprint of: Pawłowski Ł., Bartmański M., Mielewczyk-Gryń A., Zieliński A., Chitosan/poly(4-vinylpyridine) coatings formed on AgNPs-decorated titanium, MATERIALS LETTERS Vol. 319 (2022), 132293, DOI: 10.1016/j.matlet.2022.132293

Chitosan/poly(4-vinylpyridine) coatings formed on AgNPs-decorated titanium

Łukasz Pawłowski[a*], Michał Bartmański[a], Aleksandra Mielewczyk-Gryń[b], Andrzej Zieliński[a]

Faculty of Mechanical Engineering and Ship Technology[a]; Faculty of Applied Physics and Mathematics[b]; Gdańsk University of Technology, Narutowicza 11/12, 80-233 Gdańsk, Poland; micbartm@pg.edu.pl (M.B.), alegryn@pg.edu.p (A.M.G); azielins@pg.edu.pl (A.Z.)

* Corresponding author: lukasz.pawlowski@pg.edu.pl (Ł.P.); Tel.: +48-883-797-081

Abstract: Electrophoretic deposition (EPD) of chitosan/poly(4-vinylpyridine) (chit/P4VP) coatings on titanium substrates previously decorated with silver nanoparticles (AgNPs) was performed at different content of P4VP in the suspension and different voltage values. The results revealed that the composite coatings were formed, well-adjacent to the titanium substrate, of suitable roughness, hydrophilicity, and corrosion resistance. The voltage value and P4VP content had complex and different effects on coating properties, due to the effects of process parameters on microstructure and adhesion. The best coatings of both chitosan and P4VP were formed at 10 V at 0.1% (w/w) during a one-minute deposition. These pH-sensitive antibacterial coatings may, based on the present results, be recommended for surface modification of titanium implants.

Keywords: thin films; chitosan; poly(4-vinylpyridine); silver nanoparticles; electrophoretic deposition; corrosion;

1. Introduction

The most attractive antibacterial pH-sensitive coatings of titanium implants studied so far were those based on chitosan able to degrade in a wide pH range, dopped with nanosilver. Due to the tendency of chitosan to swell in aqueous media, e.g. the simulated body fluid, the need for a natural/synthetic hybrid biopolymer blend emerged [1-5]. Among other compounds, poly(4-vinylpyridine) (P4VP) can be considered as pH-related species dissolving at pH<5 [6-8]. The coatings composed of such two polymers demonstrating different relationships of degradation rate on pH value can be effective over a wide range of low pH typical of inflammation states. Despite this advantage, such composite was seldom tested, e.g. as a hybrid material for (waste) water treatment [9], and not as a coating. Therefore, this research has been aimed to develop chit-P4VP coatings, presumably effective in acidic, neutral, and slightly alkaline

electrolytes typical of the human body [10], and determine the effects of deposition voltage and solution composition on their microstructure, adhesion, wettability, and corrosion parameters.

2. Materials and methods

Ti Grade 2 samples (EkspresStal, Poland) were ground with sandpapers up to No. 800, then rinsed with isopropanol and distilled water. AgNPs were produced on a bare surface by $AgNO_3$ (VWR International, Belgium) electro-reduction at 0.005 g/L content and voltage of -1.2 V during 15 s. Electrophoretic deposition of coatings was performed in a suspension of 0.1% (w/w) of chitosan (purity > 99%, MW ~ 310-375 kDa, Sigma-Aldrich, USA) and either 0.1% (samples A and B) or 0.2% (w/w) (sample C) of P4VP (MW ~ 160 kDa, Sigma-Aldrich, USA) in 1% CH_3COOH (99.9%, Stanlab, Poland) at a voltage of 5 V (samples A and C), or 10 V (sample B), for 1 min. The testing procedures were based on [11,12].

The morphology of coatings was examined with SEM (JSM-7800 F, Jeol, Japan) and elemental composition by EDS (Edax Inc., USA), the coating thickness with dual scope thickness meter (SN100146594, Helmut Fischer GmbH, Germany), surface roughness by AFM (NaniteAFM, Nanosurf AG, Switzerland) on a 50×50 μm area, and wettability by the falling drop method in 10 s (Attention Theta Life, Biolin Scientific, Finland). FTIR spectrometry (ATR mode) (Perkin Elmer Frontier, USA) was used to determine chemical bonds in the coatings. Adhesion of the coatings was determined by scratch test (120 mN force, 500 μm distance, NanoTest Vantage, Micro Materials, UK).

The electrochemical corrosion tests included measurements of open-circuit potentials (OCP), potentiodynamic polarization method, and electrochemical impedance spectroscopy (EIS), in a simulated body fluid (SBF) of the composition according to the PN-EN ISO 10993-15, at 37 °C and pH 7.4, by a potentiostat (Atlas 0531, Atlas Sollich, Poland). The OCP values were determined after 1 h of exposure. The EIS investigations were taken at a frequency from 1 Hz to 100 kHz, and at the amplitude of 10 mV; the data were processed using ZView software (Scribner Associates, USA). The potentiodynamic curves were obtained in the voltage range of -1.0 to 1.0 V at a potential change rate of 1 mV/s followed by the assessment of the corrosion potential (E_{corr}) and corrosion current density (i_{corr}) utilizing the Tafel extrapolation approach.

3. Results and discussion

The SEM and EDS (Fig. 1a) showed the Ag nanoparticles (AgNPs) uniformly dispersed on the surface. The chit/P4VP coatings fully covered the substrate decorated with AgNPs (Fig. 1b). The

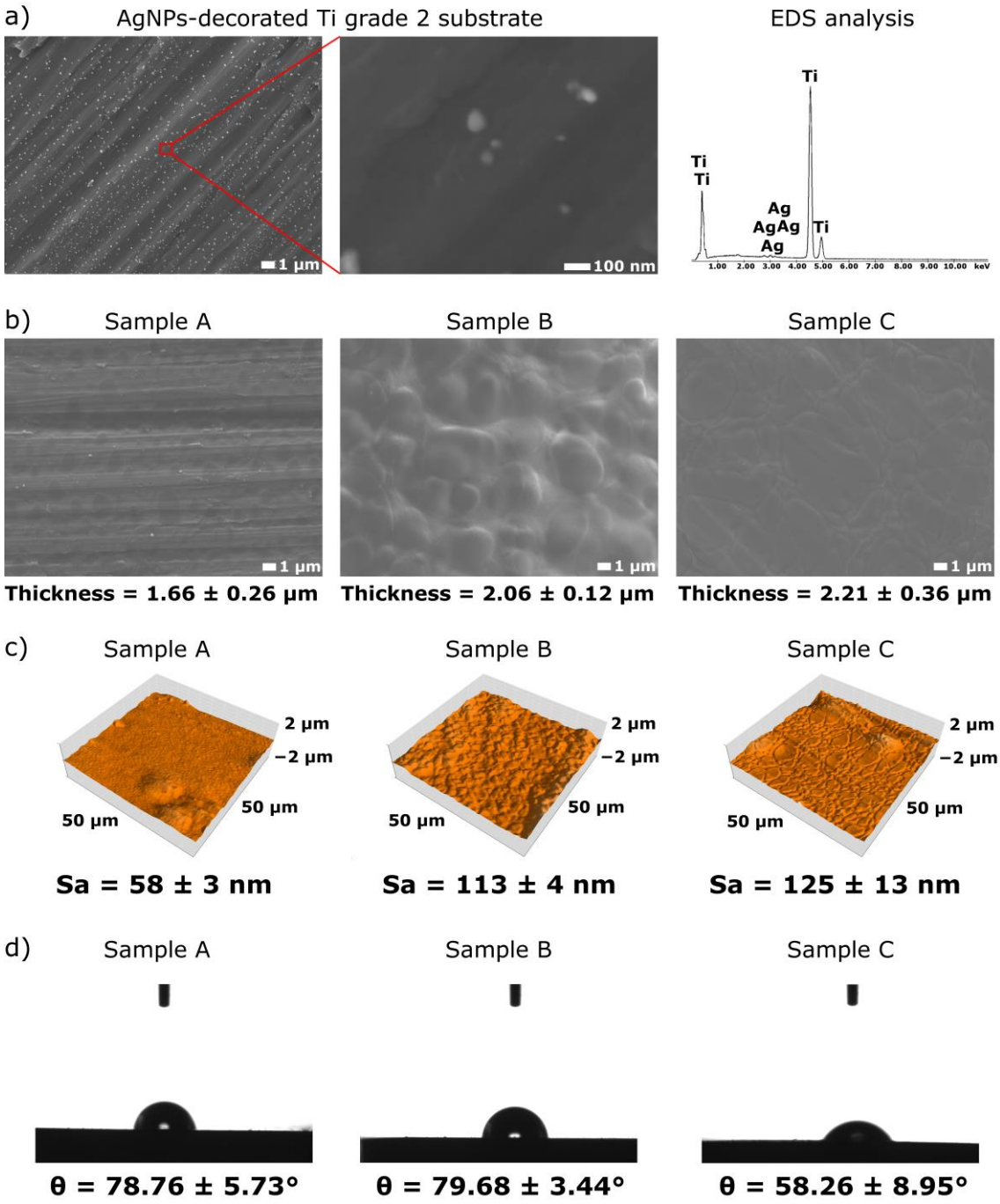

Figure 1. a) SEM and EDS results for AgNPs-decorated surface; b) SEM images and thicknesses (n=10) for chit/P4VP coatings; c) AFM topography maps and Sa values (n=3); d) water drop images and contact angle values (n=5).

increasing both the P4VP content in the bath and the deposition voltage resulted in greater thickness of the coating (Fig. 1b). Furthermore, both variables made the coating rougher due to faster water electrolysis and more hydrogen bubbles on the cathode at higher voltage, and greater misfit of both polymer components

with increasing P4VP amount, relatively (Fig. 1c). All coatings were hydrophilic (Fig. 1d), with wettability slightly increasing with voltage and more pronouncedly decreasing with PV4P amount.

The FTIR spectrum was made for sample B only (Fig. 2a). The vibrations characteristic of the pyridine ring present in the P4VP molecule [13] appears at 1598, 1556, 1461, and 1415 cm^{-1}. Less intense bands characteristic for chitosan are also visible. The band at 3450 cm^{-1} is attributed to $–NH_2$ and –OH groups stretching vibration. The peaks characteristic for the chitosan appeared at 1657 cm^{-1} (due to $CONH_2$), at 1080 cm^{-1} (C-O bond), and 1598 cm^{-1} (amine group) [14,15]. The FTIR results confirm then that coating composed of both polymers has been present on the surface after EPD.

All the coatings demonstrated corrosion parameters close to each other and resistivity much better than that of bare surface; as the time course of OCP (Fig. 2b) indicates the electrochemical reaction rate, while the OCP magnitude discloses the corrosion tendency [16], the equilibrium is quickly attained and all coatings are tight. The drastic decrease in i_{corr} (determined by Tafel extrapolation of the curves in Fig. 2c) after each coating deposition confirms their protective properties (Table 1); the rising PV4P content makes the coating less uniform reflecting in higher corrosion rate. The equivalent electrical circuits (Fig. 2d) here used were already described in [4], and the χ^2 value in the range of 10^{-3}–10^{-4} suggests a satisfactory fitting. According to the Nyquist (Fig. 2e) and Bode plots (Fig. 2f), both increasing voltage and P4VP content resulted in decreasing impedance, but increasing resistance (Table 1). The electrochemical results can be explained by thickness increasing with voltage (better protection) which is worsened by a greater amount of a second coating component due to less tight structure resulting in the easier appearance of corrosion channels.

As illustrated (Fig. 2g) by the friction force - normal force relationships during the scratch test, the mean critical forces L_c (Table 1) resulting in coating delamination increased with rising voltage and lowered with increasing P4VP content.

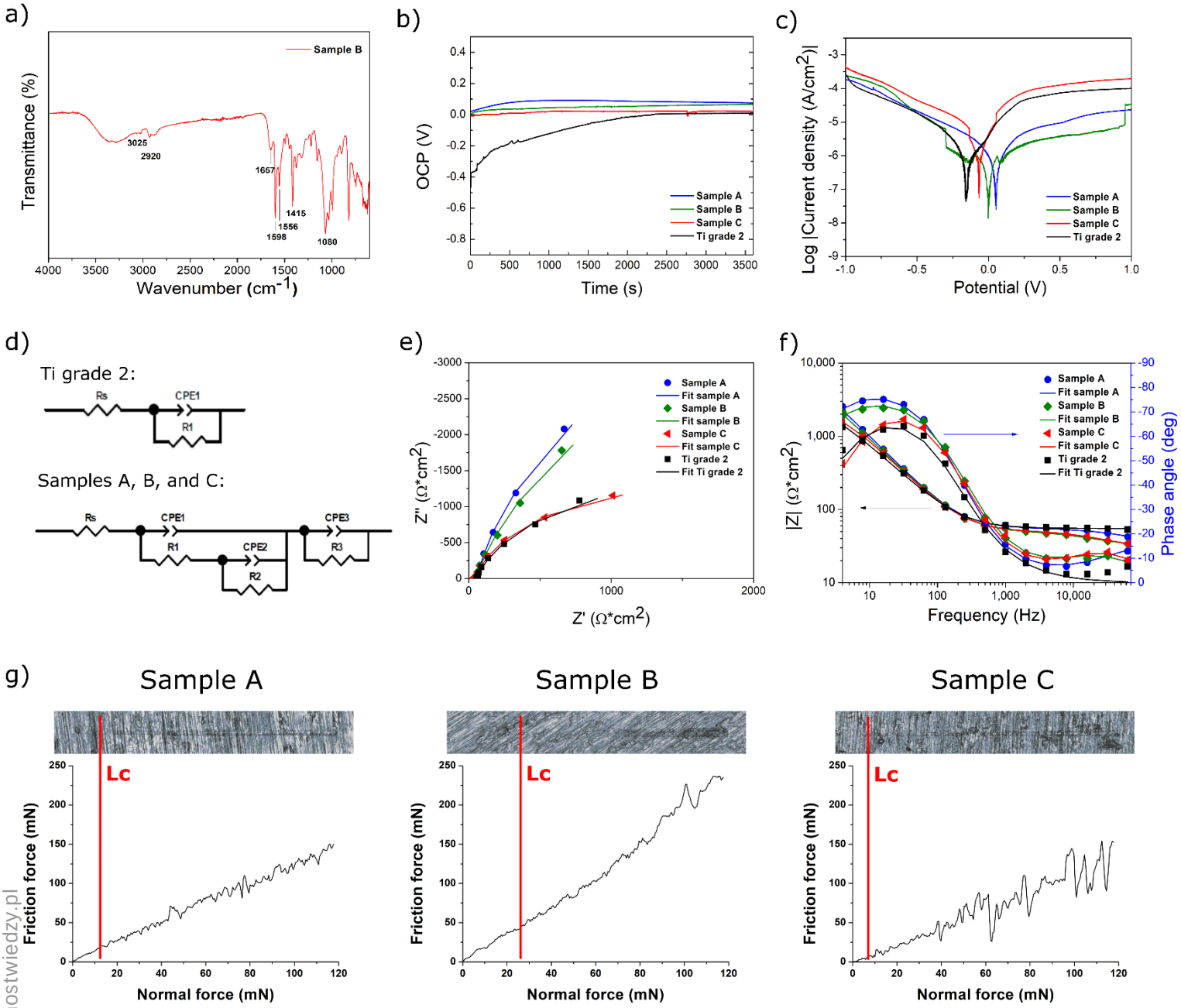

Figure 2. Results of: a) FTIR analysis for sample B, and electrochemical studies: b) OCP characteristics, c) potentiodynamic relationships; d) equivalent circuits used, e) Nyquist plots, and f) Bode-phase and Bode-Z plots; g) scratch test runs with shown scratch (top) and marked critical load L_c (bottom).

The obtained results can be explained by the effects of process parameters on microstructure. The increasing voltage makes the coating thicker, less permeable, and highly adhesive to the substrate. On the other hand, the growing P4VP content results in the greater mechanical misfit between macromolecules of softer and harder polymers and, likely, weaker adhesion and less tight coating followed by increasing

corrosion. It seems that, at a smaller amount of P4VP, a higher voltage is preferable as more ions/molecules are transferred to an electrode in a time unit, and this coating seems denser/more compact.

Table 1. Results of corrosion and scratch-crack tests (n=10).

Sample	OCP (V)	E_{corr} (V)	i_{corr} (A/cm^2)	R_s (Ohm)	χ^2 (-)	L_c (mN)
Ti (bare substrate)	0.009	- 0.147	30.719	54.93	0.00992	-
A	0.074	0.068	0.858	23.23	0.00076	12.28±3.19
B	0.065	0.004	0.458	30.22	0.00182	27.09±5.51
C	0.019	- 0.065	5.044	30.02	0.00134	7.78±2.47

4. Conclusions

The composite coatings chit/P4VP on Ag-decorated Ti surface of good adhesion and several properties can be obtained by EPD in a suspension containing 0.1-0.2% (w/w) of each substance, respectively, at voltage 5-10 V for 1 min. The most profitable among all here investigated is the coating deposited at 10 V and 0.1% (w/w) of P4VP content.

The voltage growing from 5 to 10 V results in increasing roughness, wettability, OCP, resistivity, scratch-crack resistance, and decreasing current density and impedance. The increasing P4VP amount, from 0.1 to 0.2% (w/w) leads to increasing roughness, resistivity, impedance, and corrosion current, and decreasing wettability, OCP, and scratch-crack resistance. The observed effects can be attributed to changes in microstructure, thickness, roughness, tightness, and adhesion of the coatings.

Acknowledgments

The research received financial support from the Gdańsk University of Technology. Our deep gratitude to Aleksandra Laska, and Dr. Grzegorz Gajowiec.

References

[1] B. Tyliszczak, A. Drabczyk, S. Kudłacik-Kramarczyk, K. Bialik-Wąs, R. Kijkowska, A. Sobczak-Kupiec, Preparation and cytotoxicity of chitosan-based hydrogels modified with silver nanoparticles. Colloids and Surfaces B: Biointerfaces. 160 (2017) 325–330. https://doi.org/10.1016/j.colsurfb.2017.09.044.

[2] R. Socrates, O. Prymak, K. Loza, N. Sakthivel, A. Rajaram, M. Epple, S. Narayana Kalkura, Biomimetic fabrication of mineralized composite films of nanosilver loaded native fibrillar collagen and chitosan, Mater. Sci. Eng. C. 99 (2019) 357–366. https://doi.org/10.1016/j.msec.2019.01.101.

[3] N.T.P. Nguyen, L.V.H. Nguyen, N. T. Thanh, V.V. Toi, T.N. Quyen, P.A. Tran, H.M.D. Wang, T.H. Nguyen, Stabilization of silver nanoparticles in chitosan and gelatin hydrogel and its applications, Mater. Lett. 248 (2019) 241–245. https://doi.org/10.1016/j.matlet.2019.03.103.

[4] Ł. Pawłowski, M. Bartmański, A. Mielewczyk-Gryń, B.M. Cieślik, G. Gajowiec, A. Zieliński, Electrophoretically Deposited Chitosan/Eudragit E 100/AgNPs Composite Coatings on Titanium Substrate as a Silver Release System, Materials (Basel). 14 (2021) 4533. https://doi:10.3390/ma14164533.

[5] L. Ren, Y. Zhao, L. Yang, W. Cao, H. Wang, X. Lian, X. Gao, B. Niu, W. Li, Preparation and characterization of the catechol functionalized chitosan-Ag NPs deposited onto titanium surface, Surf. Coat. Techn. 420 (2021) 127319. https://doi.org/10.1016/j.surfcoat.2021.127319.

[6] A.K. Mishra, J. Lim, J. Lee, S. Park, Y. Seo, H. Hwang, J.K. Kim, Control drug release behavior by highly stable and pH sensitive poly (*N*-vinylpyrrolidone)-*block*-poly(4-vinylpyridine) copolymer micelles, Polymer. 213 (2021) 123329. https://doi.org/10.1016/j.polymer.2020.123329.

[7] M. Atif, K. He, M. Irfan, Y. Wang, F. Hu, L. Chen, Y. Wang, pH responsive switchable protein adsorption properties of poly (2-methyl-2-oxazoline)/ poly(4-vinyl pyridine) based coatings: Influence of poly(4-vinyl pyridine) chain length and ionic strength, Progr. Organic Coat. 157 (2021) 106307. https://doi.org/10.1016/j.progcoat.2021.106307.

[8] A. Alshhab, E. Yilmaz, Sodium alginate/poly(4-vinylpyridine) polyelectrolyte multilayer films: Preparation, characterization and ciprofloxacin HCl release, Intl. J. Biol. Macromolecules. 147 (2020) 809–820. https://doi.org/10.1016/j.ijbiomac.2019.10.058.

[9] X. Solimando, P. Champagne, M.F. Cunningham, Synthesis of Biohybrid Particles by Modification of Chitosan Beads via RAFT Polymerization in Dispersed Media. Mater. Sci. Eng. 14 (2020) 1–10. https://doi:10.1002/mren.202000029.

[10] Pattanashetti, N.A.; Heggannavar, G.B.; Kariduraganavar, M.Y. Smart Biopolymers and their Biomedical Applications. Procedia Manuf. 2017, 12, 263–279.

[11] Ł. Pawłowski, M. Bartmański, G. Strugała, A. Mielewczyk-Gryń, M. Jażdżewska, A. Zieliński, Electrophoretic Deposition and Characterization of Chitosan/Eudragit E 100 Coatings on Titanium Substrate, Coatings. 10 (2020) 607. https://doi.org/10.3390/coatings10070607.

[12] M. Nycz, K. Arkusz, D.G. Pijanowska, Influence of the silver nanoparticles (AgNPs) formation conditions onto titanium dioxide (TiO2) nanotubes based electrodes on their impedimetric response, Nanomaterials. 9 (2019) 1072. https://doi.org/10.3390/nano9081072.

[13] Y. Xue, H. Xiao, Antibacterial/Antiviral Property and Mechanism of Dual-Functional Quaternized Pyridinium-type Copolymer, Polymers. 7 (2015) 2290-2303. https:// doi:10.3390/polym7111514.

[14] C. Lustriane, F.M. Dwivany, V. Suendo, M. Reza, Effect of chitosan and chitosan-nanoparticles on post-harvest quality of banana fruits, J. Plant Biotechnol. 45 (2018) 36-44. https://doi.org/10.5010/JPB.2018.45.1.036.

[15] S. Anicuta, L. Dobre, M. Stroescu, I. Jipa, Fourier Transform Infrared (ftir) spectroscopy for characterization of antimicrobial films containing chitosan, An. Univ. Orad. Fasc.: Ecotoxic., Zootehn., Tehn. Ind. Aliment. (2010) 1234-1240.

[16] Łosiewicz, B.; Maszybrocka, J.; Kubisztal, J.; Skrabalak, G.; Stwora, A. Corrosion resistance of the cpti g2 cellular lattice with tpms architecture for gas diffusion electrodes. Materials 2021, 14, 81.